Chromosome Research (2006) 14:477–495
DOI: 10.1007/s10577-006-1075-0

Genome-wide scanning of HoxB1-associated loci in mouse ES cells using an open-ended Chromosome Conformation Capture methodology

Hugo Würtele[1,3] & Pierre Chartrand[2,3]*
[1]*Molecular Biology Program, Université de Montreal, CP 6128, succ. Centre-ville, Montréal, Québec, H3C 3J7, Canada;* [2]*Department of Pathology and Cellular Biology, Université de Montreal, CP 6128, succ. Centre-ville, Montréal, Québec, H3C 3J7, Canada;* [3]*Institute for Research in Immunology and Cancer, Université de Montreal, CP 6128, succ. Centre-ville, Montréal, Québec, H3C 3J7, Canada; Tel: +1-514-343-7354; Fax: +1-514-343-7780; E-mail: pierre.chartrand@umontreal.ca*
**Correspondence*

Received 1 March 2006. Received in revised form and accepted for publication by Wendy Bickmore 5 May 2006

Key words: chromatin folding, chromosomal territories, Chromosome Conformation Capture, HoxB1, megabase loop model, nuclear organization

Abstract

Spatial proximity between genomic loci can play important roles in their function and regulation. We have developed an open-ended method based on Chromosome Conformation Capture technology allowing us to perform a genome-wide scan of the loci that form the spatial environment of a given locus at a given time. As a proof of principle we present the use of this methodology to investigate the dynamics of the spatial environment of the HoxB1 gene before and after the induction of its expression in mouse embryonic stem cells. Our results indicate that the HoxB1 locus' immediate spatial environment can be divided roughly into three parts: a first part is represented by a domain of immediate proximity on each side of the HoxB1 locus covering approximately 110 kb, a second part extends to a domain of 800 kb and a third part consists of distal intra-chromosomal and inter-chromosomal interactions. Consistent with FISH studies showing the decondensation and repositioning of HoxB1 outside of its chromosomal territory during its expression, the proportion of inter-chromosomal interactions between HoxB1 and the rest of the genome increases after its induction, while interactions with distal intra-chromosomal loci become less frequent. These results indicate that this technique can be used to determine the dynamics of loci interactions on a genome-wide scale.

Introduction

The genetic material is organized at many levels in the nucleus and this organization is related to nuclear functions such as replication, gene expression and DNA repair (reviewed in Lamond & Earnshaw 1998 and Cremer & Cremer 2001). It is thus increasingly clear that the spatial proximity between genomic loci can have important consequences on their functions. For example, the mouse beta-globin complex adopts a specific folding in erythroid cells, in which non-contiguous regulatory sequences are clustered in the nuclear space with the intervening sequences looped out. The genes of the complex are then sequentially recruited to these regulatory sequences during their expression (Carter *et al.* 2002, Tolhuis *et al.* 2002, de Laat & Grosveld 2003, Palstra *et al.* 2003, Patrinos *et al.* 2004). Active genes located megabases away from each other can also co-localize to share a 'transcription factory' (Osborne *et al.*

2004). Finally, distant intra- and inter-chromosomal loci involved in recurrent translocations are frequently in close spatial proximity in the nuclei of relevant cell types (Nikiforova *et al.* 2000, Roix *et al.* 2003, Parada *et al.* 2004).

Because of the fact that chromatin movement and dispersion in the nuclear volume are restricted (Marshall *et al.* 1997, Chubb *et al.* 2002; reviewed in Gasser 2002), the spatial environment of a locus can only consist of a limited fraction of the genome. The higher-order organization of the chromosomes is directly involved in the definition of this environment. Indeed, chromosomes occupy distinct territories in the nuclear space, with little inter-chromosomal mingling (reviewed in Cremer & Cremer 2001) and the localization of these territories relative to one another and to nuclear structures is relatively stable during interphase (Gerlich *et al.* 2003, Walter *et al.* 2003). While the positioning of chromosomes one relative to another appears to be mostly random (Cornforth *et al.* 2002), many reports have shown that preferential inter-chromosomal associations exist (Nagele *et al.* 1999, Roix *et al.* 2003, Parada *et al.* 2004).

Chromosomal arms and bands also occupy distinct spatial territories (Dietzel *et al.* 1998), suggesting that the higher-order folding of the chromatin has an impact on the spatial proximity of loci at a sub-chromosomal scale. This is also suggested by the fact that the relationship between the interphase distance of two given loci and their genomic separation has been shown by FISH to be biphasic: the average spatial distance between loci increases rapidly with their genomic separation until 1–2 mb, at which point the increase becomes less pronounced (Yokota *et al.* 1995). These observations have led to the proposal of a model in which independent mb-sized loops with random internal organization are arranged on an undefined structure following a 'random-walk' behavior (Sachs *et al.* 1995, Yokota *et al.* 1995). Based on computer simulations and experimental evidence, a 'multi-loop subcompartment' model was subsequently proposed in which the mb-sized domains are internally organized in smaller sub-loops of about 120 kb (Münkel *et al.* 1999).

Interestingly, the spatial distance between loci with respect to their genomic separation is less important in regions of compacted chromatin such as G-bands than in more open regions such as R-bands (Yokota *et al.* 1997), showing that the local chromosomal landscape of a given locus can modulate its spatial environment. The presence of genes in particular is known to influence this environment. While transcription foci can be distributed within the interior of chromosomal territories (Verschure *et al.* 1999, Mahy *et al.* 2002a), gene-rich regions are often found near the periphery or outside of their territories in a gene density and transcription-dependent manner (Mahy *et al.* 2002b). Large-scale chromatin decondensation of gene-containing loci and their relocalization relative to their chromosomal territories have also been linked to transcriptional activity. For example, the HoxB1, beta-globin and major histocompatibility complex genes are relocated outside of their respective chromosomal territories before or during their expression, which results in important changes to their spatial environment (Volpi *et al.* 2000, Ragoczy *et al.* 2003, Chambeyron & Bickmore 2004).

Nucleotide-level investigation of chromatin spatial organization has been made possible by the development of methods such as RNA trap (Carter *et al.* 2002) and Chromosome Conformation Capture (Dekker *et al.* 2002). However, in these methodologies the investigator has to hypothesize beforehand which genomic loci are likely to be in close spatial proximity to a locus of interest. We have developed an open-ended method based on the Chromosome Conformation Capture technology allowing us to determine without *a-priori* knowledge which genomic loci form the spatial neighborhood of a given locus. Here, we describe the use of this methodology to investigate the dynamics of the HoxB1 gene during the induction of its expression in the context of retinoic acid-induced differentiation of mouse embryonic stem (ES) cells. We show that both intra- and inter-chromosomal loci are accessible to the HoxB1 locus. Interactions between HoxB1 and its chromosome were found to be separated in distinct domains of differential accessibility to the gene. We also show that inter-chromosomal loci become more accessible to HoxB1 upon the induction of its expression, which is consistent with the extrusion of the gene from its chromosomal territory.

Material and methods

Mouse embryonic stem cells culture and differentiation

Undifferentiated OS25 mouse embryonic stem cells were graciously provided by W. Bickmore's laboratory. They were maintained in 0.1% gelatin-coated dishes in Dulbecco modified Eagle medium (DMEM) supplemented with 10% fetal calf serum (FCS), non-essential amino acids, 0.3 mg/ml L-glutamine, 0.15 mM A-monothioglycerol (MTG), 1000 U/ml murine LIF (Chemicon International ESGRO), 100 μg/ml G418, and were kept in a 5% CO_2 atmosphere at 37°C. The medium of undifferentiated cells was changed daily. These undifferentiated cells were labeled 'Day 1'. The differentiation protocol was performed as described previously (Chambeyron & Bickmore 2004). Briefly, 5×10^5 cells were plated in uncoated tissue culture dishes using the same medium as before but without LIF and G418 for 1 day (Day 0); 5×10^{-6} M retinoic acid (RA) was then added to this medium for 4 days (Day 1 to 4). After 2 days of RA treatment the medium was supplemented with 2.5 μM ganciclovir for 2 days (until Day 4 of the time course). Subsequently, the medium was only supplemented with ganciclovir (no RA) for 3 days (Day 5 to 7). The medium was changed every 2 days of the differentiation protocol.

RT-PCR analysis

Total RNA was extracted using Trizol (Invitrogen). Between 500 ng and 5 μg of total RNA was treated with 1 U of RNase free DNAse I (Invitrogen). cDNA were generated using 200 U of M-MLV-Reverse Transcriptase (Invitrogen) and 5 ng/μl of random hexanucleotides (Invitrogen). Semi-quantitative and real-time RT-PCR (Figure 1) were then performed using 1/20 of the cDNA preparation per PCR. Primer sequences: Oct4: 5′-ggcgttctctttggaaaggtgttc-3′ and 5′-ctcgaaccacatccttctct-3′; HoxB1: 5′-ccatatcctccgccg cag-3′ and 5′-cggactggtcagaggcatc-3′; β-actin: 5′-ggtcagaaggactcctatgtgg-3′ and 5′-tctcagctgtggtggt gaag-3′. Semi-quantitative PCR was performed using 1 U of Taq polymerase per reaction and the following cycling conditions: 2 min at 94°C; 15 s at 94°C, 30 s at 60°C, 45 s at 72°C for 25 cycles (β-actin) or 35 cycles (HoxB1 and Oct4); 5 min at 72°C. Real-time PCR was performed in duplicate, using a Stratagene Mx3000P machine, the companion software MxPro (Stratagene) and the Quantitect SYBR green PCR kit (Qiagen). Cycling conditions were similar to those used for the semi-quantitative approach, except that the number of cycles was set at 40 for all amplifications. Standard curves for each primer pair were generated using 1:10, 1:100 and 1:1000 dilutions of a Day-1 cDNA preparation.

Chromosome Conformation Capture (3C)

A slight modification of the 3C procedure published by Tolhuis and collaborators was used, except for the PCR step (Tolhuis *et al.* 2002; see below). Briefly,

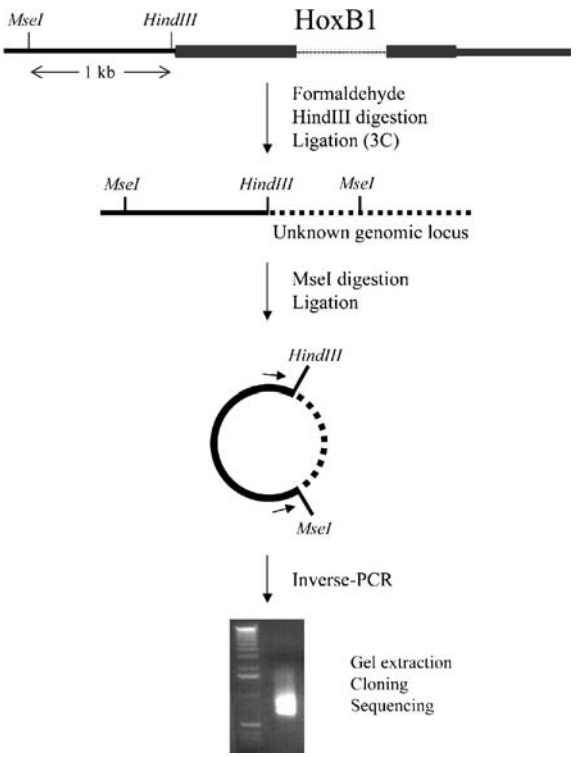

Figure 1. The inverse-PCR 3C method based on the Chromosome Conformation Capture (3C) technology developed by Dekker *et al.* (2002). Loci that are frequently in close spatial proximity to the starting locus (in this case HoxB1) are crosslinked and ligated to it at high frequency, resulting in more frequent inverse-PCR amplification and cloning. The HindIII restriction site used in the 3C part of the method is located 16 bp upstream of the HoxB1 gene.

between 5×10^5 and 5×10^6 cells were washed with phosphate buffered saline (PBS) and treated with DMEM/10% FBS supplemented with 2% formaldehyde for 10 min at room temperature. Formaldehyde was then quenched with 1 M glycine and the cells were recovered by scraping with a rubber policeman. Cells were pipetted up and down to obtain a single-cell suspension. Nuclei were then extracted in the presence of protease inhibitors and treated overnight with 600 U of HindIII restriction enzyme (New England Biolabs). The digested chromatin was then ligated using T4 DNA ligase (New England Biolabs) in dilute conditions (2.5 ng/μl). Crosslinks were reversed by overnight incubation at 65°C with proteinase K. DNA was then extracted and submitted to PCR.

Inverse-PCR procedure

3C-treated DNA was digested with the MseI restriction endonuclease (New England Biolabs). Digested DNA was then phenol:chloroform extracted and ligated in dilute conditions (2.5 ng/μl) using T4 DNA ligase (New England Biolabs). Inverse-PCR on the HoxB1 locus was performed using the Expand High Fidelity PCR system (Roche) and between 50 and 200 ng of MseI and ligase treated 3C templates. A first PCR was performed using primers 387F (5′-ATGGGGGTTCTGGGATAAGTAA-3′) and 317R (5′-GGGACAAAAGGATGACTAGGAAGGGAGAG-3′); 1/50 of this first PCR was then used in a second PCR amplification using nested primers 548F (5′-TTGGGAGGGGAGTAAAAGTCTT-3′) and

Table 1. Inverse-PCR 3C performed on the HoxB1 locus

Day of time course	DNA template[a]	PCR name	No. of pooled PCR[b]	No. of clones[c]
D−1	B1	A	1	94
D−1	B1	B	1	86
D−1	B1	C	1	60
D−1	B1	D	1	77
D−1	B1	E	1	77
D−1	B1	F	1	23
D−1	B1	1–9	9	70
D−1	B1	10–18	9	66
D−1	F1	H	1	58
D−1	F1	N	1	60
D−1	F1	1–9	9	72
D−1	F1	10–18	9	82
D−1	F1	19–27	9	78
D1	F2	I	1 78	
D1	F2	J	1	88
D1	F2	1–10	10	77
D1	F2	11–20	10	80
D1	F2	21–30	10	77
D1	F3	1–7	7	87
D1	F3	8–14	7	82
D1	F3	15–21	7	83
D3	E1	1–10	10	68
D3	E1	11–20	10	77
D3	E1	21–28	8	77
D3	E1	29–36	8	64
D3	E1	37–44	8	71
D3	E1	45–52	8	57
D3	G1	1–9	9	146
D3	G2	1–9	9	165

[a]Each DNA template was prepared from an independent retinoic acid time course.
[b]Number of independent inverse-PCR pooled before cloning.
[c]Number of clones that were successfully sequenced and/or located in genome databases.

269R (5′-CAGGGTGTGAGCCAGGGGTCTAAA ATC-3′) to obtain enough PCR products for subsequent cloning steps. PCR conditions were as follows: 2 min at 94°C; 15 s at 94°C, 30 s at 60°C, 3 min at 68°C for 10 cycles; 15 s at 94°C, 30 s at 60°C, 3 min + 5 s/cycle auto extension at 68°C for 20 cycles; 5 min at 68°C. Table 1 describes the different inverse-PCR that were cloned and sequenced. In some instances multiple independent inverse-PCRs were pooled before cloning to ensure the sequencing of a broad diversity of products from each cloning experiment.

PCR products cloning

PCR products were separated by agarose gel electrophoresis. DNA was extracted from gel fragments using the Sephaglas Bandprep kit (Amersham Pharmacia Biotech) and cloned using the Qiagen A-addition and PCR cloning kit (Qiagen). Ligation products were then transformed in DH5alpha electrocompetent bacteria (Invitrogen). Blue/white selection using X-gal was used to identify clones containing an insert. Plasmid DNA was extracted using standard techniques or by performing a PCR designed to amplify the inserts on positive bacterial colonies.

Sequences analyses

Sequences were analyzed using UCSC Genome Browser at http://genome.ucsc.edu/ (Mouse genome assembly of March 2005) and the Ensembl Karyoview at http://www.ensembl.org/.

Classical 3C analyses

Eight proximal HindIII genomic fragments were chosen to perform classical 3C analyses (labeled −143122, −66631, −30994, −17379, 5631, 12515, 36214 and 53223 in Figure 3). Control DNA templates containing the HoxB1 locus HindIII genomic fragment ligated to the chosen loci were generated by PCR using a primer specific for the HoxB1 locus and another primer specific for the genomic HindIII fragment of interest. The relative copy number of each of these control template preparations was then quantified by Taqman quantitative PCR using primers and a probe located within their common HoxB1 region (a five log standard curve was generated for this primer pair and probe to permit an accurate comparison of the relative copy number of the different control templates). These quantified control templates were serially diluted over four log and used to generate standard curves by quantitative PCR using a primer and Taqman probe specific to the HoxB1 locus and a primer specific to the locus of interest. To simulate the sequence complexity found in the 3C templates, 100 ng of mouse genomic DNA was added to each of these standard curve reactions. These standard curves allowed us to correct for differences in amplification efficiencies of the different primer pairs and thus to normalize the signals obtained in the amplifications performed on the actual 3C templates. The same primer pairs and probe were used to quantify the abundance of the ligation products in Day −1 and Day 3 3C templates by comparing the signal obtained with the normalized standard curves. To adjust for differences in 3C efficiencies and quantity of DNA of each 3C template, the quantitative PCR data of each template was normalized by comparing the signal obtained for a given primer pair to the signal obtained for the 5631 locus. This allowed us to calculate the 3C signals obtained for each locus relative to 5631 value in independent 3C templates. The mean of these relative 3C signals is presented in Figure 4. Quantifications were performed at least in duplicate using the Applied Biosystems Inc. Taqman master mix, a Stratagene Mx3000P real-time PCR machine with its companion software MxPro and an Applied Biosystems Inc. 7900HT machine with the companion SDS 2.2.2 software. Conditions for the Taqman quantitative PCR were 10 min at 94°C; 15 s at 94°C, 1 min at 60°C for 50 cycles.

3C efficiency control

The beta-actin locus was chosen to perform the 3C efficiency control (see Figure 7 and text for details). The frequency of crosslinking of the HindIII genomic fragment containing the beta-actin gene to its adjacent upstream HindIII fragment was quantified. First, a 25 cycle PCR was performed on the 3C templates using primers ActNestA: 5′-ACTTAGGTG TACCTGTGTGTGCCT-3′ and ActAdj: 5′-AGCA GTGGTTTCTATTGGCTGTCG-3′. This first PCR was performed using the Expand High Fidelity PCR kit from Roche Diagnostics. PCR conditions were as follows: 2 min at 94°C; 20 s at 94°C, 30 s at

60°C, 1 min at 72°C for 25 cycles. SYBR green quantitative PCR was performed on 1/50 of this first amplification using the nested primer ActA: 5′-CTTCTGACCTAGAACTCTTGATCCC-3′ and the ActAdj primer using the same PCR conditions except for the number of cycles which was set at 35 in this case. A standard curve was made for the SYBR green quantitative PCR using four log serial dilutions of the 25 cycle PCR products and primers ActA and ActAdj. To compare the copy number of the genomic HindIII fragment containing the beta-actin gene in the different 3C templates (and thus the quantity of DNA present in each 3C template preparations), a standard curve was made using serial dilutions (four log) of mouse genomic DNA and primers ActA, ActB: 5′-CCCTCTACACACAC TCAGAATTCATC-3′ and Taqman probe ActS: 5′-CGGGGAACGGTACCACACTCAGTTT-3′. Conditions for this Taqman quantitative PCR were 10 min at 94°C; 15 s at 94°C, 1 min at 60°C for 50 cycles. This PCR amplifies a fragment located within the HindIII genomic fragment containing the beta-actin gene. The same PCR was performed on each of the 3C templates and the signal was compared to the standard curve to obtain the copy number of this fragment in each 3C template. This copy number was used to normalize the signal representing the cross-linking of the HindIII genomic fragment containing the beta-actin gene to its adjacent fragment located immediately upstream in the different 3C template. Quantifications were performed at least in duplicate using the Applied Biosystems Inc. Taqman master mix or the Qiagen Quantitect SYBR green master mix and a Stratagene Mx3000P real-time PCR machine with its companion software MxPro.

Results

Experimental design

The purpose of this study was to develop a method that would allow the characterization of the spatial genomic neighborhood of a locus of interest in mammalian cells. To achieve this we modified the Chromosome Conformation Capture (3C) methodology originally described by Dekker and collaborators (Dekker *et al.* 2002). In this method cells are treated with a formaldehyde solution, which results in the chemical crosslinking of genomic loci that are in close spatial proximity in the nuclear space. Crosslinked nuclei are treated with a restriction enzyme and the digested chromatin is ligated in dilute conditions, which favors the ligation of crosslinked molecules over random inter-molecular ligation. The frequency of ligation of two DNA fragments is thus proportional to the frequency at which they are in close spatial proximity in the nuclei of the cell population analyzed. Finally, crosslinks are reversed, DNA is extracted and the ligated products are analyzed by PCR. In the standard 3C procedure the abundance of specific ligation products is determined by quantitative PCR. We sought to expand this technique by replacing the directed quantitative PCR with an open-ended inverse-PCR allowing the amplification of unknown sequences ligated to the locus of interest. These inverse-PCR products can then be cloned and sequenced to determine their genomic localization. Loci that are frequently in close spatial proximity to the locus of interest are thus amplified and cloned more frequently from the inverse-PCR than loci that are rarely in close spatial proximity to this locus.

As a proof of principle of this methodology we characterized the spatial genomic environment of the HoxB1 gene during the induction of its expression in the context of retinoic acid-induced differentiation of OS25 mouse embryonic stem (ES) cells. The OS25 mouse ES cell line was chosen because it was used previously in the characterization of the large-scale decondensation and repositioning of the HoxB1 locus

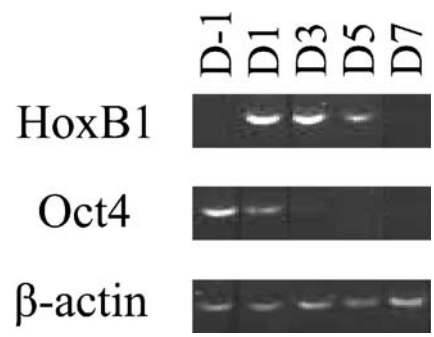

Figure 2. RT-PCR quantification of the expression of HoxB1, OCT4 and β-actin genes during the retinoic acid-induced differentiation of mouse OS25 ES cells. Each lane refers to a different day (D) of the retinoic acid time-course (see Material and methods).

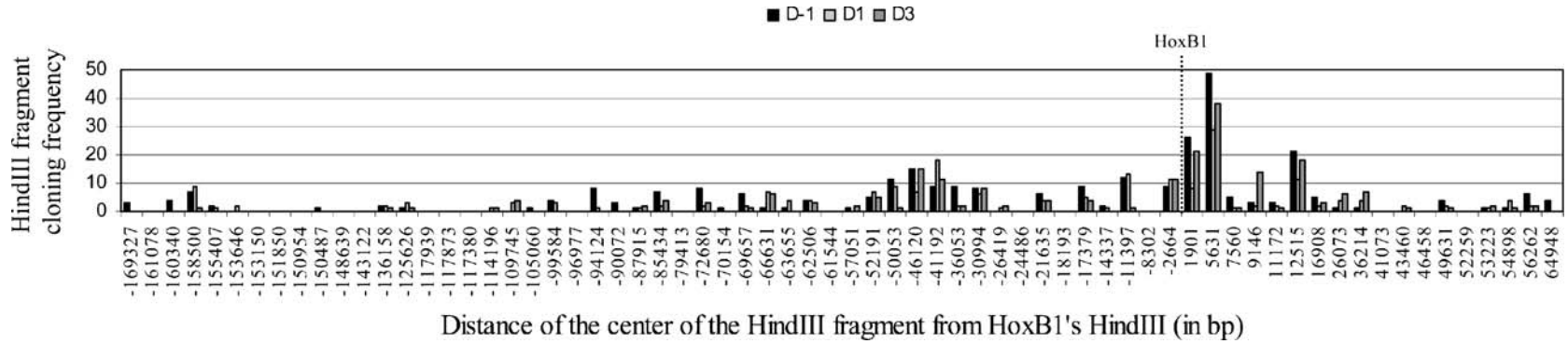

Figure 3. Cloning frequency of genomic HindIII fragments proximal to the HoxB1 locus. Since a given HindIII fragment can be ligated from either of its ends to HoxB1's HindIII site, two distinct inverse-PCR fragments can be generated from any given HindIII fragment. The distance of the center of each genomic HindIII fragment from the HoxB1 HindIII site used in the inverse-PCR 3C experiments is indicated. Negative distances represent loci located in 5′ of the HoxB1 locus while loci located in 3′ are represented by positive distances. This graph is not drawn to scale. The fragment labeled −2664 comes from the recircularization of the starting locus on itself and should thus not be considered as a bona-fide crosslinking event.

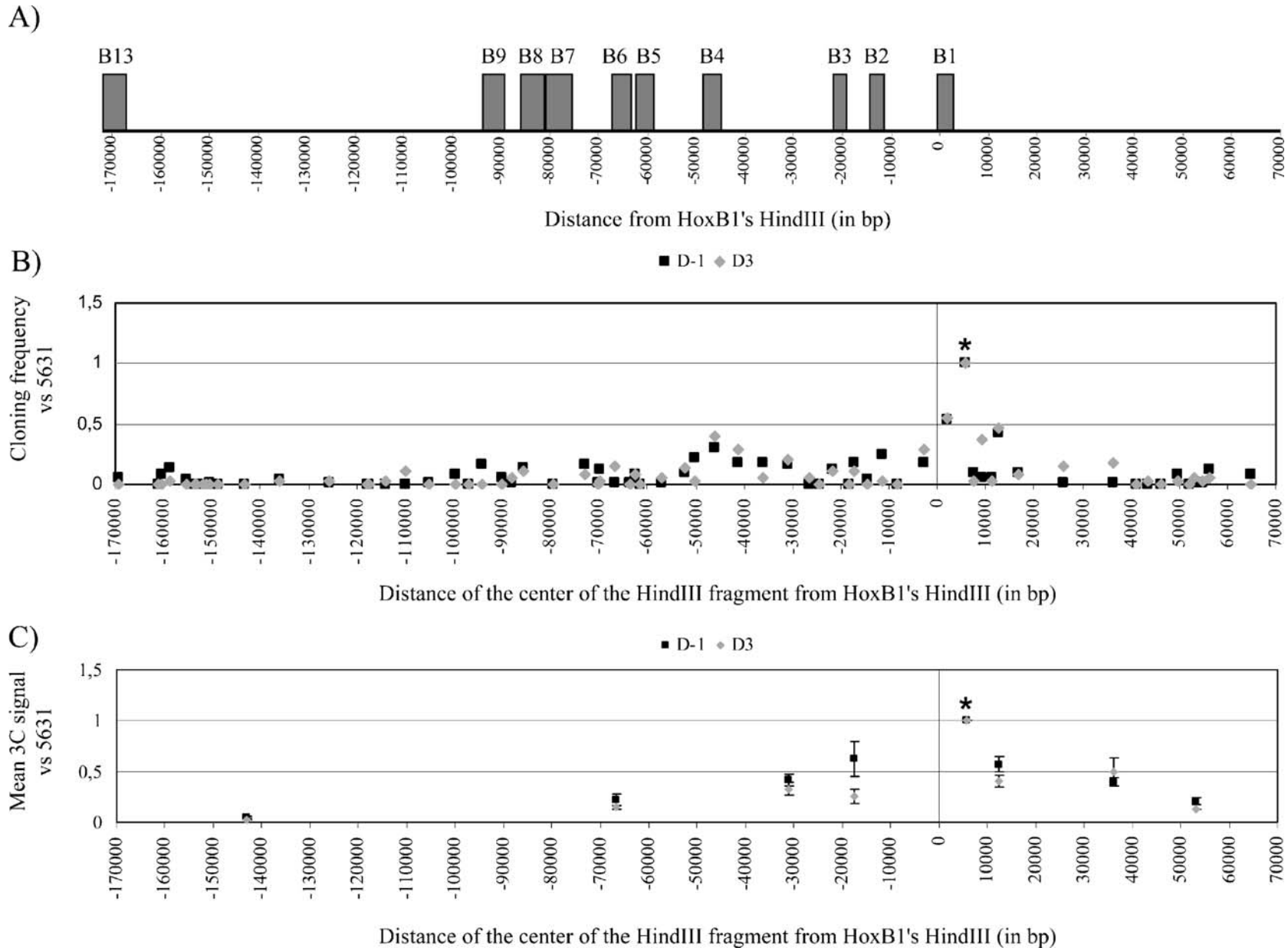
A)
B13
B9 B8 B7
B6 B5
B4
B3 B2
B1
-170000 -160000 -150000 -140000 -130000 -120000 -110000 -100000 -90000 -80000 -70000 -60000 -50000 -40000 -30000 -20000 -10000 0 10000 20000 30000 40000 50000 60000 70000
Distance from HoxB1's HindIII (in bp)
B)
D-1 D3
Cloning frequency vs 5631
1,5
1
0,5
0
*
-170000 -160000 -150000 -140000 -130000 -120000 -110000 -100000 -90000 -80000 -70000 -60000 -50000 -40000 -30000 -20000 -10000 0 10000 20000 30000 40000 50000 60000 70000
Distance of the center of the HindIII fragment from HoxB1's HindIII (in bp)
C)
D-1 D3
Mean 3C signal vs 5631
1,5
1
0,5
0
*
-170000 -160000 -150000 -140000 -130000 -120000 -110000 -100000 -90000 -80000 -70000 -60000 -50000 -40000 -30000 -20000 -10000 0 10000 20000 30000 40000 50000 60000 70000
Distance of the center of the HindIII fragment from HoxB1's HindIII (in bp)

relative to its chromosomal territory upon induction of its expression by retinoic acid (Chambeyron & Bickmore 2004). The inverse-PCR 3C experiments were performed as illustrated in Figure 1. A HindIII restriction site located 16 bp upstream of the HoxB1 gene was used for the 3C part of the experiment (formaldehyde treatment, HindIII digestion, ligation) while an MseI site located 1 kb upstream of the HindIII site was used as the inverse-PCR restriction site. MseI is a 'frequent cutter' possessing a 4 bp recognition site: the use of this restriction enzyme should limit the size of the inverse-PCR products and facilitate their amplification. Figure 1 shows an agarose gel electrophoresis of a representative inverse-PCR 3C experiment. As expected, a smear is obtained from this type of PCR; as many different loci are crosslinked to the HoxB1 locus and are amplified by this method, the resulting PCR products are of various sizes. It can be noted that most products are between 650 bp and 1 kb in length (650 bp is the minimal possible size for an inverse-PCR product because of the position of the PCR primers used relative to the MseI restriction sites). They are thus of similar size and should be amplified at comparable efficiencies. These PCR products are then cloned and sequenced, and their genomic location is determined using genome databases.

Consistent with previous reports, Figure 2 shows that HoxB1 expression is strongly induced after 1 day of retinoic acid treatment, remains high at Day 3 and is gradually lost by Day 5. Oct4 gene expression was used as a control: as has been shown previously and in contrast to HoxB1, this gene is strongly expressed in undifferentiated cells and repressed after treatment with retinoic acid (Chambeyron & Bickmore 2004). Quantitative real-time PCR analysis confirmed an at least 60- and 40-fold enrichment in HoxB1 transcripts at Day 1 and 3 respectively of the differentiation protocol as compared to untreated cells (data not shown). Inverse-PCR 3C was thus performed at Day −1 (before retinoic acid treatment and HoxB1 gene expression) and Day 1 and 3 (after 1 or 3 days of retinoic acid treatment respectively and during HoxB1 gene expression). Table 1 details the various inverse-PCR performed on each day of the retinoic acid time course (see Material and methods for details). For each day between 653 and 904 clones were recovered and sequenced, and their genomic location was determined using genome databases (UCSC Mouse BLAT; http://genome.ucsc.edu).

Proximal loci are recovered at high frequency by inverse-PCR 3C

Both intra- and inter-chromosomal crosslinking partner loci were cloned from the inverse-PCR 3C experiments. Proximal intra-chromosomal loci were first analyzed in more detail. Cloning frequencies of the HindIII genomic fragments surrounding the HoxB1 locus are shown in Figures 3 and 4B. Because of their linear proximity with HoxB1, we expected that proximal loci would be recovered at high frequency in our screening. Concordant with these expectations, almost every locus located within 40 kb in 3′ and 70 kb in 5′ of the HoxB1 locus was recovered at least once (only four out of these 31 proximal HindIII fragments were not recovered). The data presented in Figures 3 and 4B suggest that, globally, crosslinking frequencies are higher for loci located within these proximal genomic regions and that beyond this interval the crosslinking partners become more sparsely distributed and are recovered generally less frequently. As we will document in more detail below, this suggests that the spatial environment of the HoxB1 gene can be separated in distinct genomic regions of accessibility. These figures also show that the frequency recovery of the crosslinking partners decreases more slowly with distance in the 5′ proximal region of the gene than in

Figure 4. Classical 3C analysis of proximal genomic HindIII fragments. **A**: Localization of the HoxB cluster genes. **B**: Cloning frequencies of individual genomic HindIII fragments surrounding the HoxB1 gene relative to fragment 5631 (highlighted with a star (*)). Only Day −1 and Day 3 data are presented. The distances of the center of each genomic HindIII fragment from the HoxB1 HindIII site used in the inverse-PCR 3C experiments is displayed. **C**: Classical 3C analysis of the genomic interval displayed in Figures 3 and 4B. 3C signals are normalized to the signal representing the crosslinking of HoxB1 to the genomic HindIII fragment located 5631 bp in 3′ of the gene (highlighted with a star (*); see Material and methods for details). The mean of these relative signals is presented. Error bars: ± standard error of the mean. The distance of the center of each genomic HindIII fragment from the HoxB1's HindIII site used in the 3C experiments is displayed. Negative distances represent loci located in 5′ of the HoxB1 locus while loci located in 3′ are represented by positive distances. The HindIII genomic fragments that were used are labeled −143122, −66631, −30994, −17379, 5631, 12515, 36214 and 53223 in Figure 3.

the 3′ one. Globally, most of the proximal fragments also appeared to be recovered at similar relative frequencies on the different days of the time course, which suggests that the accessibility of the gene to its proximal spatial environment is not importantly modified by the retinoic acid treatment.

From the results presented in Figure 3, it is apparent that some HindIII fragments were recovered more frequently than others. For example, the fragments labeled 5631, 12515 and −30994 were cloned frequently in our screen, while other proximal and distal fragments were either recovered at low frequency or not at all (for example −57051, −8302 and 11172). While this could reflect real differences in crosslinking frequencies with HoxB1, the analysis of individual HindIII fragments is complicated by the fact that a low cloning frequency could be the result of an inefficient amplification by the inverse-PCR procedure. To address this possibility we determined the size of the inverse-PCR products resulting from the proximal HindIII fragments (located within 70 kb in 5′ and 40 kb in 3′; data not shown). This analysis showed that most of the infrequently recovered fragments were probably poorly suited for the inverse-PCR: either they did not possess an MseI site or they would result in larger inverse-PCR products. This suggests that some genomic fragments cannot be efficiently recovered by the inverse-PCR 3C methodology irrespective of their frequency of crosslinking to HoxB1.

Because of this, we wanted to verify if, globally, the inverse-PCR 3C results were compatible with classical 3C analyses. Figure 4C shows the results of a classical 3C analysis of the crosslinking frequencies of selected HindIII genomic fragments proximal to the HoxB1 locus. In general there is a good agreement between the two methods as both the density of recovered crosslinking partners within a genomic region and their cloning frequency seem to be closely correlated to the frequencies of crosslinking observed by classical 3C analysis (compare Figure 4B and C). By considering each side of the starting locus independently, it can be seen that the 3C crosslinking frequencies of the first three 3′ and first two 5′ proximal HindIII genomic fragments are similar among themselves. However, loci that are located more distally (for example loci −143122 and 53223) are clearly crosslinked less frequently than the other loci located on the same side of HoxB1.

Globally, there is also good agreement between the cloning frequency of individual HindIII genomic fragments by inverse-PCR 3C and their classical 3C crosslinking frequency. It is noteworthy that the fragment that was recovered most frequently from the inverse-PCR 3C screening (labeled 5631 in Figure 3) was also the most frequently crosslinked fragment by classical 3C. Concordant with inverse-PCR 3C data, the crosslinking frequencies of the investigated HindIII fragments are also generally similar at Day −1 and 3, except for the fragment located 17379 bp in 5′ of HoxB1, which seems to be crosslinked somewhat less frequently at Day 3 than at Day −1 by classical 3C. This fragment was also cloned slightly less frequently at Day 3 than at Day −1 during the inverse-PCR 3C experiments. While this difference in cloning frequency is not statistically significant, this suggests that a larger-scale screening could in some cases identify more subtle differences in crosslinking frequency.

There can also be some differences at the level of individual HindIII fragments, which was to be expected since, as explained above, some fragments cannot be efficiently recovered by the inverse-PCR 3C method. For example, the fragment 36214 located in 3′ of the gene was not cloned as frequently as the 12515 fragment, but appears to be crosslinked to HoxB1 at a similar frequency by 3C analysis. However, a bioinformatic analysis revealed that the 36214 HindIII fragment could be recovered mostly from one of its ends using inverse-PCR 3C since the other end would have resulted in a long inverse-PCR product. It is thus clear that, when considering individual genomic fragments, results obtained by inverse-PCR 3C should be validated by classical 3C analysis.

The nuclear environment of the HoxB1 gene can be separated in distinct genomic domains of spatial interactions

Figure 5 shows the cumulative proportion of the clones of crosslinking partners recovered at various genomic distances from the HoxB1 HindIII site used in our experiments. The proportions were obtained by dividing the number of clones representing crosslinking partners located within a given distance from HoxB1, by the total number of clones recovered for

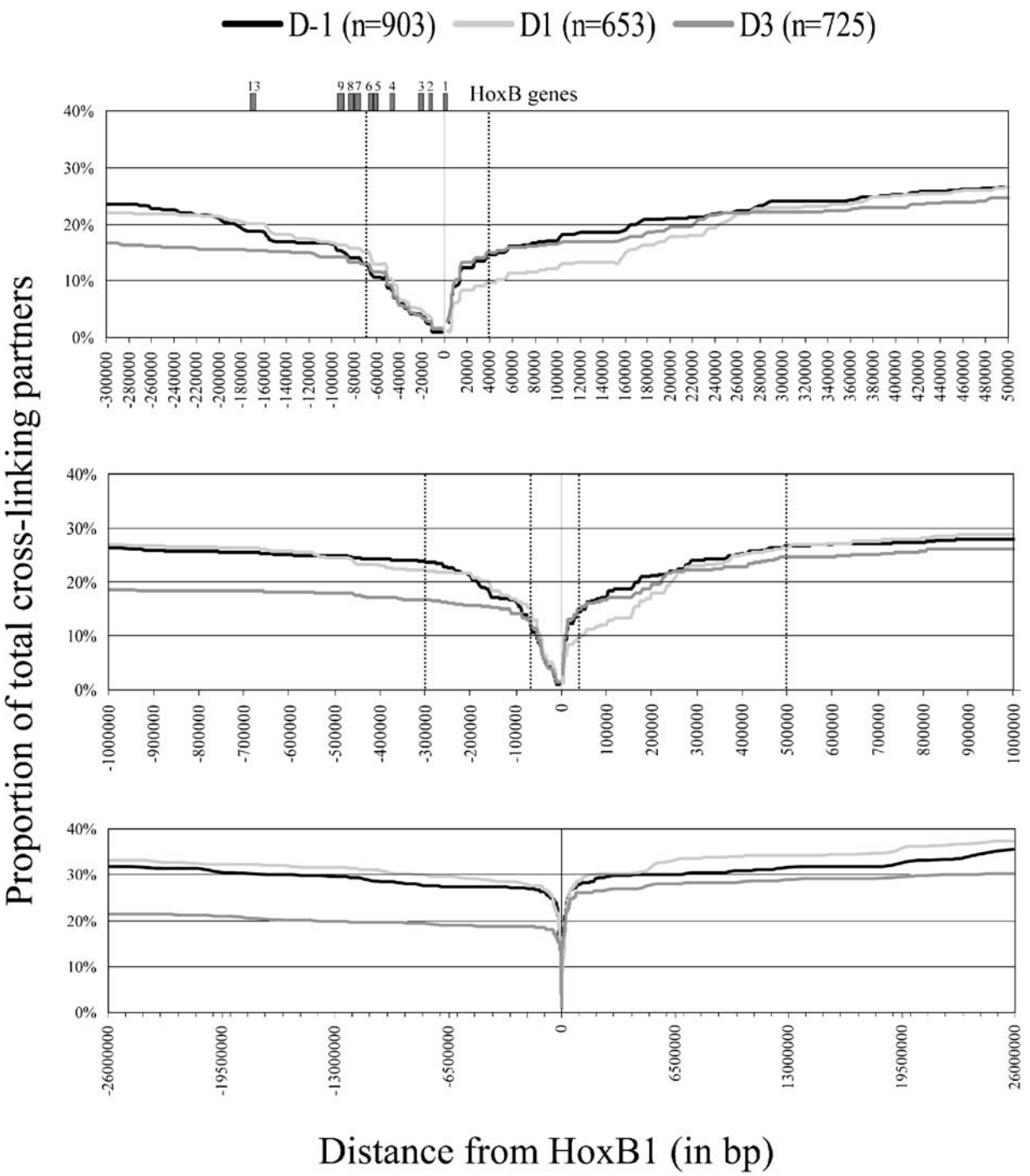

Figure 5. Cumulative proportion of total crosslinking partners recovered at various distances from the HoxB1 locus. Proportions are obtained by dividing the number of recovered clones of crosslinking partners located between a given genomic location and the HoxB1 HindIII site used in the inverse-PCR 3C experiments by the total number of clones recovered for each day of the time course. Negative distances represent loci located in 5′ of the HoxB1 locus while loci located in 3′ are represented by positive distances. Dashed lines delineate particular regions of the curves (see text). The genomic localization of the genes of the HoxB cluster is also presented.

each day of the retinoic acid treatment. This curve thus allows the description of the accumulation of clones of crosslinking partners over large genomic regions and takes into account both the density of crosslinking partners and their frequency of recovery by inverse-PCR 3C. Based on the fact that the curve is changing abruptly at specific genomic distances from HoxB1, and on the data presented in Figures 3 and 4, we separated the curve in distinct regions displaying different rates of accumulation of clones of crosslinking partners. The steepness of the curve in the genomic regions encompassing approximately 70 kb in 5′ and 40 kb in 3′ indicates that these regions possess a high density of crosslinking partners that are recovered frequently by inverse-PCR 3C. In the 5′ 70 kb proximal genomic region the curve appears to be linear, indicating a high density of crosslinking partners and a rate of accumulation of clones that is mostly independent of their linear genomic distance from HoxB1. This suggests that many of the loci that are located within this region are frequently crosslinked to HoxB1 and that the crosslinking frequencies are diminishing more slowly with distance from HoxB1 in this region than in the 3′ region. Indeed, in the proximal 40 kb region in 3′ of the gene, the curve is clearly logarithmic in nature, which suggests that the frequency of crosslinking is rapidly decreasing with distance within this genomic interval.

After these proximal regions the rate of accumulation of clones diminishes, which means that the density of partners, as well as their frequency of cloning, is lower than those of the proximal domains. However, the fact that the curve is still steep indicates that there is a relatively high density of crosslinking partners in these regions until another breakpoint, which is located at approximately 300 kb in 5′ and 500 kb in 3′. This portion of the curve is also logarithmic: the probability of being crosslinked to HoxB1 is thus decreasing with genomic distance until the 5′ 300 kb and 3′ 500 kb boundaries. After these distances the rate of accumulation of clones drops importantly, and the curve appears to be roughly linear for the rest of the distance measured. The probability of being crosslinked to HoxB1 thus appears to be more stable over great genomic distances after the 5′ 300 kb and 3′ 500 kb boundaries, which results in a more sparse distribution of the crosslinking partners and reduced frequencies of recovery. As we will see in Figure 8, the accessibility to HoxB1 appears to decrease with genomic separation even after the 5′ 300 kb and 3′ 500 kb boundaries; however, the fact that this decrease is very progressive results in a curve that looks linear in Figure 5. While the domains described above seem to exist irrespective of the expression status of the HoxB1 gene, their relative importance varies in

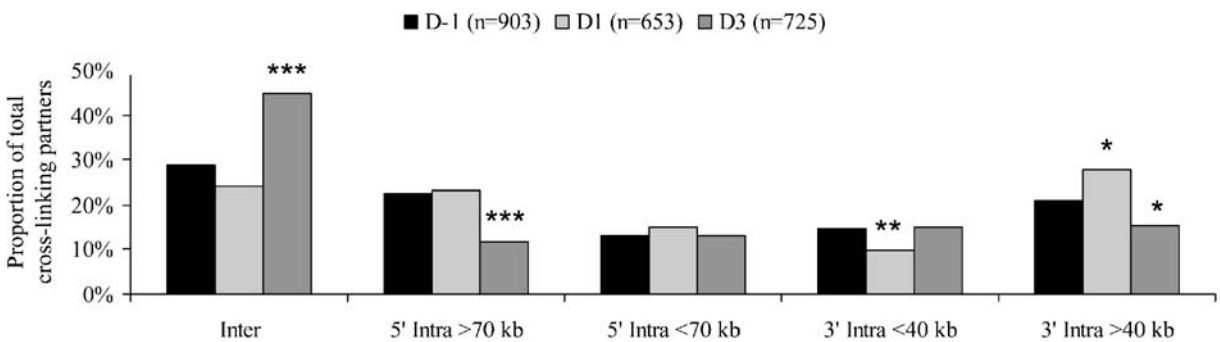

Figure 6. Distribution of cloned crosslinking partners of the HoxB1 gene in different genomic intervals. Proportions represent the number of recovered clones of crosslinking partners located within a given genomic interval divided by the total number of clones recovered for a given day of the time course. Inter: inter-chromosomal partners. 5′ intra > 70 kb: intra-chromosomal partners located farther than 70 kb in 5′ of the HoxB1 HindIII site used in the inverse-PCR 3C. 5′ intra < 70 kb: intra-chromosomal partners located within 70 kb in 5′ of HoxB1's HindIII site. 3′ intra < 40 kb: intra-chromosomal partners located within 40 kb in 3′ of HoxB1's HindIII site. 3′ intra > 40 kb: intra-chromosomal partners located farther than 40 kb in 3′ of HoxB1's HindIII site. ***: significantly different from Day −1 value ($p < 0.0001$; Pearson's chi-square test). **: significantly different from Day −1 value ($p = 0.0097$; Pearson's chi-square test). *: significantly different from Day −1 value ($p = 0.015$; Pearson's chi-square test).

relation to expression; these differences are the focus of the next section.

The spatial genomic environment of the HoxB1 gene changes during retinoic acid treatment of mouse ES cells

The analysis presented in Figure 5 suggests that the distribution of the clones of crosslinking partners within the different genomic domains of accessibility to the HoxB1 locus is not equivalent at each day of the retinoic acid treatment time course. For example, the crosslinking partners located in the distal domains located in 5′ of HoxB1 appear to be recovered noticeably less frequently at Day 3 than at Day −1 or Day 1 of the time course. Figure 6 shows the proportion of the recovered clones of crosslinking partners falling within any of five genomic regions defined according to the analyses described above.

The proximal 5′ 70 kb and 3′ 40 kb regions were found to contain in total approximately 25–28% of the recovered clones at each day of the time course, thus suggesting that in general the accessibility of HoxB1 to these proximal domains is not importantly modified by its expression status. Intriguingly, however, crosslinking partners located in the 3′ proximal domain represent a significantly lower proportion of the total recovered clones at Day 1 than at Day −1 (p = 0.0097, Pearson's chi-square test), which seems to be linked to a higher proportion of partners in the distal 3′ intra > 40 kb compartment (p = 0.015; Pearson's chi-square test).

As was suggested by the results presented in Figure 5, there is a significantly smaller proportion of clones located in the 5′ and 3′ distal regions (5′

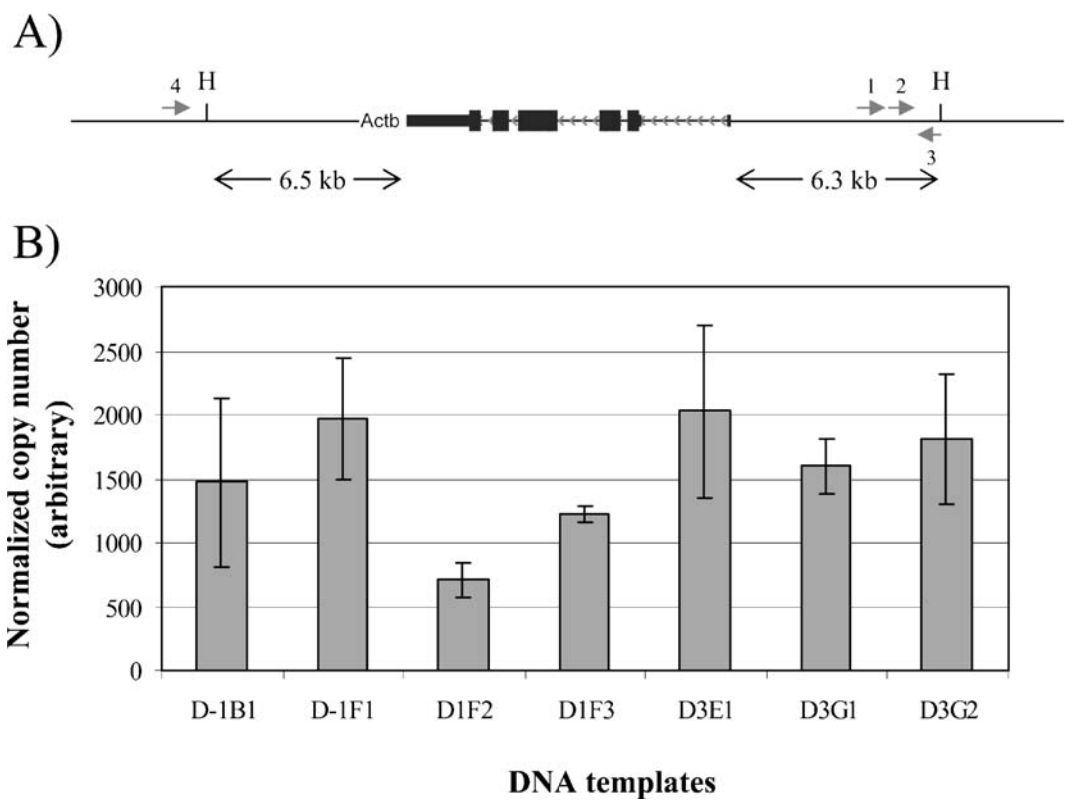

Figure 7. Crosslinking efficiency control. See text for details. **A**: Configuration of the beta-actin locus. The gray arrows marked 1, 2 and 4 represent the PCR primers that were used to amplify the ligation products resulting from the crosslinking of the adjacent HindIII fragments. The gray arrows marked 2 and 3 represent the primers that were used to normalize the 3C signal according to the quantity of DNA. Not drawn to scale. **B**: Results of the experiment described in **A**. The 3C signal (obtained using primers 1, 2 and 4) was normalized using the genomic quantity signal (obtained using primers 2 and 3). The name of the 3C templates refers to Table 1. Normalized copy numbers were arbitrarily defined to allow comparison of the crosslinking signal. Error bars: ± standard error of the mean.

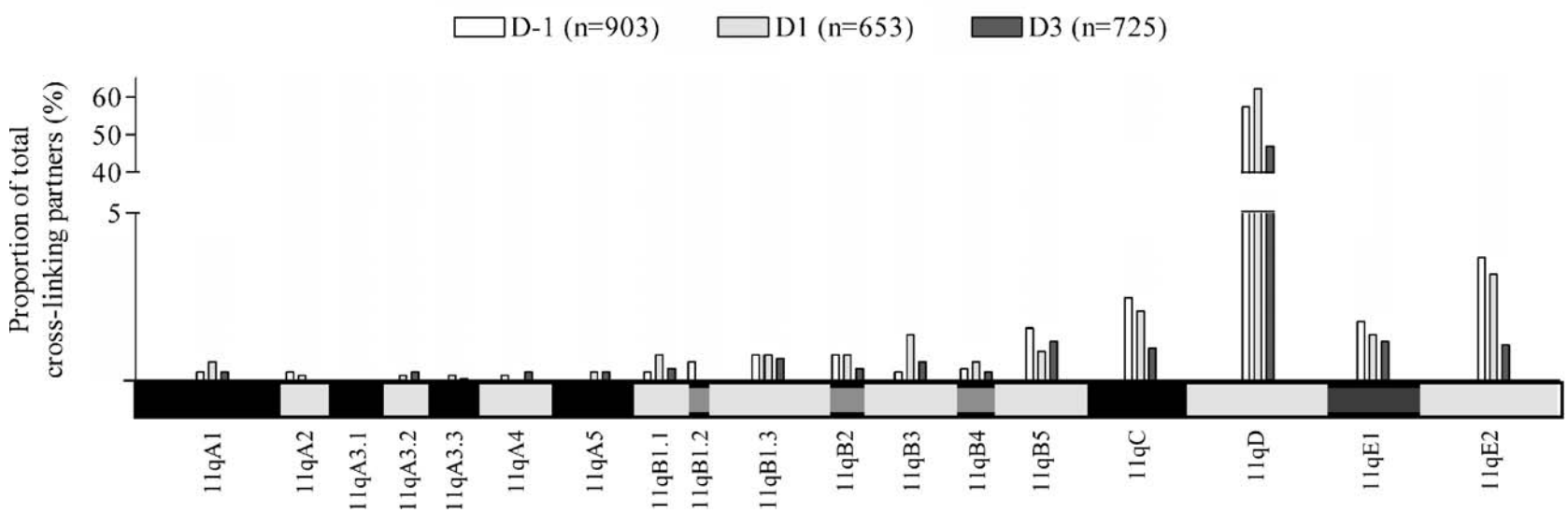

Figure 8. Intra-chromosomal band distribution of the proportion of total cloned crosslinking partners. Proportions are calculated by dividing the number of clones of crosslinking partners located in a given band by the total number of clones recovered for each day of the time course. The HoxB1 locus is located in band 11qD.

intra > 70 kb and 3′ intra > 40 kb) at Day 3 than at Day −1 ($p < 0.0001$ and $p = 0.015$, respectively; Pearson's chi-square test). In fact, these regions contained in total 44% and 51% of all recovered clones at Day −1 and Day 1 respectively, whereas they contained only 27% of the Day 3 clones. It is noteworthy that this difference is much more significant for the 5′ distal genomic regions than for the 3′ one. Interestingly, concordant differences in the proportion of inter-chromosomal crosslinking partners are observed between Day 3 and Day −1. Inter-chromosomal interactions represented a minority of events (about 25–30%) at Day −1 and Day 1. In contrast, they were recovered almost as frequently as intra-chromosomal ones at Day 3 (45% of total partners) and thus significantly more frequently than at Day −1 ($p < 0.0001$; Pearson's chi-square test). These results are in agreement with the extrusion of the HoxB1 locus outside of its chromosomal territory after retinoic acid treatment of ES cells (Chambeyron & Bickmore 2004).

One possible explanation for these observations would be that the crosslinking efficiency of the 3C procedure is somehow diminished at Day 3 relative to Day −1 or Day 1, and that this reduced 3C efficiency would result in an increased amount of random ligation events. These random events would be expected to mainly involve inter-chromosomal HindIII genomic fragments, and their recovery by inverse-PCR 3C could lead to an overestimation of the inter-chromosomal interactions frequency. To evaluate if there were in fact important differences in the crosslinking efficiency of the 3C protocol between the different DNA templates used in the inverse-PCR 3C procedure, we performed the control experiment described in Figure 7A. The aim of this experiment was to compare the crosslinking frequency of two adjacent HindIII genomic fragments between each of the different DNA templates. The beta-actin gene locus was chosen for these experiments, since its expression profile is not modified by the retinoic acid treatment as confirmed by comparison to the expression profile of the housekeeping gene GAPDH (data not shown). The beta-actin gene is also on a different chromosome than the HoxB gene cluster. Thus, the crosslinking frequency of these two adjacent HindIII fragments should not be modified during the retinoic acid treatment except if there is an effect of the differentiation protocol on the crosslinking efficiency. The quantitative PCR signal obtained from the ligation of the adjacent crosslinked HindIII fragments was normalized to a signal reflecting the quantity of DNA in each 3C templates (PCR primers were chosen within the HindIII fragment containing the beta-actin gene for this quantification).

The results presented in Figure 7B demonstrate that, for a given quantity of DNA template, the signal representing the crosslinking of the adjacent beta-actin HindIII genomic fragments does not vary importantly across the different DNA templates, the largest variation being an approximately 3-fold difference between templates D3E1 and D1F2. Thus, there is no correlation between progression along the retinoic acid differentiation protocol and 3C crosslinking efficiency. These results suggest that any variation in crosslinking efficiency does not specifically affect the proportion of inter-chromosomal crosslinking partners recovered by the inverse-PCR 3C methodology and that the observed differences in the proportion of inter-chromosomal interactions between Day −1 and Day 3 are biologically relevant.

Genomic distribution of distal intra- and inter-chromosomal crosslinking partners

Figure 8 presents the distribution of cloned intra-chromosomal crosslinking partners along the entire length of mouse chromosome 11. As could be expected from the analyses presented above, the band 11qD within which the HoxB cluster is located is heavily represented in our screening. As mentioned earlier, crosslinking partners proportions appear to slowly diminish with distance from the 11qD band. No distal intra-chromosomal regions or chromosomal bands appear to be specifically associated with HoxB1, irrespective of its expression status. Inter-chromosomal crosslinking partners were also distributed among chromosomes in proportions approximately concordant with chromosome size (data not shown). The HoxB1 locus interactions with distal intra- and inter-chromosomal loci are thus consistent with randomness.

Discussion

Chromatin movements in the nuclear space are restricted (reviewed in Gasser 2002). This implies that some genomic loci are more frequently in close spatial proximity to a given locus than others. In the

present study we have used an open-ended 3C method to investigate the spatial genomic environment of the HoxB1 gene during the induction of its expression in the context of retinoic acid-induced differentiation of mouse ES cells. Our results suggest that, irrespective of its expression status, interactions between the HoxB1 locus and intra-chromosomal loci are distributed in genomic regions displaying differential accessibility to the gene. We observed that loci located within an approximately 110 kb genomic interval distributed around the HoxB1 locus are highly accessible to the gene. More distal interactions follow a biphasic distribution in which the accessibility of HoxB1 to individual genomic loci decreases with distance within an 800 kb genomic domain and becomes more or less constant in the vicinity of its 5′ 300 kb and 3′ 500 kb boundaries. This suggests that, after these distances, a great number of loci distributed over large genomic intervals are more or less equally accessible to the HoxB1 locus in a random fashion.

Results from the inverse-PCR 3C screen that we performed were generally found to be in good agreement with classical 3C analysis (Figure 4). Comparison of Figure 4B and C shows that, in general, genomic regions that are infrequently crosslinked to the HoxB1 locus were not recovered frequently by inverse-PCR 3C, and vice-versa. Two variables should be considered when comparing inverse-PCR 3C data with classical 3C: the density of crosslinking partners over a given genomic interval and their frequency of recovery. Thus, while there can be some discrepancies between the two methods on the level of individual genomic fragments, the results are remarkably compatible when considered over a larger genomic interval. This is in fact one interesting feature of the inverse-PCR 3C methodology: this method makes it possible to sample the entire genome to describe the spatial environment of a given locus and to determine which genomic regions are more likely to be in close spatial proximity to it. The frequency of crosslinking of a particular genomic fragment of interest should then be validated using classical 3C analysis.

The distribution of the clones of intra-chromosomal crosslinking partners that we obtained using inverse-PCR 3C is compatible with FISH data showing that inter-loci spatial distances follow a discontinuous relationship with regard to their genomic linear separation and with the mb-sized and multi-loop subcompartment models of chromatin folding that were derived from these observations (Sachs *et al.* 1995, Yokota *et al.* 1995, Münkel *et al.* 1999). Indeed, we observed a 110 kb preferential genomic domain within a larger 800 kb domain, which could support the presence of a sub-loop within a mb-sized domain (Münkel *et al.* 1999). Interestingly, we recovered a similar proportion of cloned partners for both the 5′ and 3′ sides of the proximal domain, but over a distance of 70 kb in 5′ and of only 40 kb in 3′. This would suggest that the position of the HoxB1 locus within this proximal domain is somewhat off-centre. The same can be said of the more distal 800 kb domain, since it extends only 300 kb in 5′ as compared to 500 kb in 3′. Our approach did not allow us to ascertain whether or not the chromatin of these domains is indeed organized as loops, but variations in local linear chromatin compaction could also result in some loci being closer and more accessible to the HoxB1 locus without necessarily invoking a loop model (Yokota *et al.* 1997).

The genomic landscape around the domain boundaries was examined. Interestingly, two retinoic acid response elements involved in the regulation of HoxB1 are located within the 3′ proximal domain, in the two HindIII fragments that were the most frequently cloned from our assay (labeled 1901 and 5631 in Figure 3; Marshall *et al.* 1996, Huang *et al.* 2002). There is also another retinoic acid response element within the HindIII fragment that was used as 'bait' in our assay. It is thus possible that the presence of these regulatory elements could be involved in the increased accessibility of the 3′ proximal domain to the starting locus. We also note that the HoxB6 gene lies within only 3 kb of the 5′ proximal domain boundary. It has been shown that the chicken HoxB gene cluster can be separated into two distinct groups: HoxB1-5 are retinoic acid sensitive whereas HoxB6-13 are regulated by fibroblast growth factor (FGF) (Bel-Vialar *et al.* 2002). An exciting possibility would be that the HoxB gene complex could be separated into functionally distinct spatial domains, with the HoxB6 gene being located at their frontier. Using the MARscan software (Rice *et al.* 2000), we also found that there were possible matrix attachment regions (MAR) near both the proximal and distal

domain boundaries. However, potential MAR sequences were also found at other genomic locations within these domains: the functional relevance of these MAR sites and the precise mechanisms involved in the formation of the accessibility domains are thus unclear at this point.

The analysis presented in Figure 6 shows that the distribution of the clones of crosslinking partners within the domains described above is influenced by the retinoic acid-induced differentiation protocol. Accessibility of HoxB1 to the proximal domain is not dramatically affected by its expression status. Nevertheless, there appears to be a slightly lower proportion of clones located in the 3′ proximal domain at Day 1 than at Day −1 or Day 3, and this seems to be concordant with an increase in accessibility to the 3′ distal domain. It is thus possible that this distal domain becomes transiently more accessible to the HoxB1 gene shortly after its induction. The accessibility of HoxB1 to distal genomic regions is more clearly affected by the retinoic acid treatment. The proportion of clones representing crosslinking partners located within the distal intra-chromosomal regions is significantly lower at Day 3 than at Day −1 or Day 1, and this diminution is translated into a higher proportion of inter-chromosomal interactions. In contrast to the situation observed at Day −1 or 1, the HoxB1 locus is thus as likely to be in close spatial proximity to inter-chromosomal loci as to intra-chromosomal ones at Day 3. These results are consistent with the reported relocalization of the HoxB1 gene outside of its chromosomal territory during retinoic acid-induced differentiation of ES cells and during mouse embryonic development (Chambeyron & Bickmore 2004, Chambeyron *et al.* 2005). It is of note that, even in undifferentiated cells, almost a third of the recovered clones are representing inter-chromosomal crosslinking partners: this could be due to the fact that, even when it is inactive, the HoxB1 gene is usually located close to the periphery of its chromosomal territory (Chambeyron & Bickmore 2004).

HoxB1 gene induction precedes the increase in the accessibility to inter-chromosomal loci in our assay, since we do not see it at Day 1 even though HoxB1 expression has been induced at that time (Figure 2). However, the relocalization of the HoxB1 gene relative to its chromosomal territory was shown by FISH to be maximal after 4 days of retinoic acid treatment, and the gene remains outside of its territory even after repression of its expression (Chambeyron & Bickmore 2004). It is also of note that chicken chromosomal territories have been reported to become more diffuse during cellular differentiation, leading to the expression-independent relocalization of many loci to more external positions of their territories (Stadler *et al.* 2004). Since 3C results represent an average of a cell population's chromosomal folding, it is possible that only after 3 days of the retinoic acid treatment does the proportion of cells in which HoxB1 is located outside of its chromosomal territory become high enough to be significant in our results.

Distal intra-chromosomal regions appear to be associated with the HoxB1 locus in a random manner, irrespective of its expression status. Inter-chromosomal crosslinking partners are also distributed across the genome in proportions consistent with randomness. While some studies have reported that stable chromosome order and organization can be shared in a cell population to some extent (Nagele *et al.* 1999, Gerlich *et al.* 2003), other results suggest that chromosome arrangements in the nuclear space are not conserved in a cell population and are thus mostly random (Cornforth *et al.* 2002, Walter *et al.* 2003). Our data are consistent with these latter observations and suggest that the HoxB1 locus can interact with a large diversity of intra- and inter-chromosomal genomic loci in the cell population studied.

One interesting possibility was that the HoxB1 gene could have been recruited to 'transcription factories' during its activation, as was demonstrated to be the case for other active genes (Osborne *et al.* 2004). We thus verified whether the crosslinking partners recovered from Day 1 and Day 3 templates were located in closer proximity to genes than those recovered from Day −1 templates, and whether these genes possessed similar functions or were functioning in related pathways. We also verified the degree of expression of these genes using available micro-array data from developing mouse embryos. The results of these analyses did not support the idea that an active HoxB1 gene is more often co-localized with other genes (active or inactive) than when it is inactive, or with genes related to a specific pathway. However, one limitation of this analysis is that the available micro-array data

(which was obtained from developing mouse embryos, and not specifically from ES cells treated with retinoic acid), may not accurately reflect the expression status of the crosslinking partners of HoxB1.

The results presented here indicate that the open-ended 3C approach that we developed makes it possible to analyze the overall spatial organization of any given locus under various conditions. The coupling of this method with DNA micro-array technologies could ultimately improve its efficiency and facilitate the high-throughput analyses of the spatial organization of genomes.

Acknowledgements

The authors acknowledge the excellent technical contribution of Edlie St-Hilaire and Jacinte Gauthier to this work. The authors also thank W. deLaat for detailed information concerning the 3C protocol, and Kevin Little for critical reading of the manuscript. H.W. is a recipient of a studentship from the Fonds de la Recherche en Santé du Québec. This work was supported by a grant from the Canadian Institutes of Health Research to P.C.

References

Bel-Vialar S, Itasaki N, Krumlauf R (2002) Initiating Hox gene expression: in the early chick neural tube differential sensitivity to FGF and RA signaling subdivides the HoxB genes in two distinct groups. *Development* **129**: 5103–5115.

Carter D, Chakalova L, Osborne CS, Dai YF, Fraser P (2002) Long-range chromatin regulatory interactions in vivo. *Nat Genet* **32**: 623–623.

Chambeyron S, Bickmore WA (2004) Chromatin decondensation and nuclear reorganization of the HoxB locus upon induction of transcription. *Genes Dev* **18**: 1119–1130.

Chambeyron S, Da Silva NR, Lawson KA, Bickmore WA (2005) Nuclear re-organisation of the Hoxb complex during mouse embryonic development. *Development* **132**: 2215–2223.

Chubb JR, Boyle S, Perry P, Bickmore WA (2002) Chromatin motion is constrained by association with nuclear compartments in human cells. *Curr Biol* **12**: 439–445.

Cornforth MN, Greulich-Bode KM, Loucas BD *et al.* (2002) Chromosomes are predominantly located randomly with respect to each other in interphase human cells. *J Cell Biol* **159**: 237–244.

Cremer T, Cremer C (2001) Chromosome territories, nuclear architecture and gene regulation in mammalian cells. *Nat Rev Genet* **2**: 292–301.

Dekker J, Rippe K, Dekker M, Kleckner N (2002) Capturing chromosome conformation. *Science* **295**: 1306–1311.

de Laat W, Grosveld F (2003) Spatial organization of gene expression: the active chromatin hub. *Chromosome Res* **11**: 447–459.

Dietzel S, Jauch A, Kienle D *et al.* (1998) Separate and variably shaped chromosome arm domains are disclosed by chromosome arm painting in human cell nuclei. *Chromosome Res* **6**: 25–33.

Gasser SM (2002) Visualizing chromatin dynamics in interphase nuclei. *Science* **296**: 1412–1416.

Gerlich D, Beaudouin J, Kalbfuss B, Daigle N, Eils R, Ellenberg J (2003) Global chromosome positions are transmitted through mitosis in mammalian cells. *Cell* **112**: 751–764.

Huang D, Chen SW, Gudas LJ (2002) Analysis of two distinct retinoic acid response elements in the homeobox gene Hoxb1 in transgenic mice. *Dev Dyn* **223**: 353–370.

Lamond AI, Earnshaw WC (1998) Structure and function in the nucleus. *Science* **280**: 547–553.

Mahy NL, Perry PE, Gilchrist S, Baldock RA, Bickmore WA (2002a) Spatial organization of active and inactive genes and noncoding DNA within chromosome territories. *J Cell Biol* **157**: 579–589.

Mahy NL, Perry PE, Bickmore WA (2002b) Gene density and transcription influence the localization of chromatin outside of chromosome territories detectable by FISH. *J Cell Biol* **159**: 753–763.

Marshall H, Morrison A, Studer M, Popperl H, Krumlauf R (1996) Retinoids and Hox genes. *FASEB J* **10**: 969–978.

Marshall WF, Straight A, Marko JF *et al.* (1997) Interphase chromosomes undergo constrained diffusional motion in living cells. *Curr Biol* **7**: 930–939.

Münkel C, Eils R, Dietzel S *et al.* (1999) Compartmentalization of interphase chromosomes observed in simulation and experiment. *J Mol Biol* **285**: 1053–1065.

Nagele RG, Freeman T, McMorrow L, Thomson Z, Kitson-Wind K, Lee H (1999) Chromosomes exhibit preferential positioning in nuclei of quiescent human cells. *J Cell Sci* **112**: 525–535.

Nikiforova MN, Stringer JR, Blough R, Medvedovic M, Fagin JA, Nikiforov YE (2000) Proximity of chromosomal loci that participate in radiation-induced rearrangements in human cells. *Science* **290**: 138–141.

Osborne CS, Chakalova L, Brown KE *et al.* (2004) Active genes dynamically colocalize to shared sites of ongoing transcription. *Nat Genet* **36**: 1065–1071.

Palstra R-J, Tolhuis B, Splinter E, Nijmeijer R, Grosveld F, de Laat W (2003) The B-globin nuclear compartment in development and erythroid differentiation. *Nat Genet* **35**: 190–194.

Parada LA, McQueen PG, Misteli T (2004) Tissue-specific spatial organization of genomes. *Genome Biol* **5**: R44.

Patrinos GP, de Krom M, de Boer E *et al.* (2004) Multiple interactions between regulatory regions are required to stabilize an active chromatin hub. *Genes Dev* **18**: 1495–1509.

Ragoczy T, Telling A, Sawado T, Groudine M, Kosak ST (2003) A genetic analysis of chromosome territory looping: diverse roles for distal regulatory elements. *Chromosome Res* **11**: 513–525.

Rice P, Longden I, Bleasby A (2000) EMBOSS: The European Molecular Biology Open Software Suite. *Trends Genet* **16**: 276–277.

Roix JJ, McQueen PG, Munson PJ, Parada LA, Misteli T (2003) Spatial proximity of translocation-prone gene loci in human lymphomas. *Nat Genet* **34**: 287–291.

Sachs RK, van den Engh G, Trask B, Yokota H, Hearst JE (1995) A random-walk/giant loop model for interphase chromosomes. *Proc Natl Acad Sci USA* **92**: 2710–2714.

Stadler S, Schnapp V, Mayer R *et al.* (2004) The architecture of chicken chromosome territories changes during differentiation. *BMC Cell Biol* **5**: 44.

Tolhuis B, Palstra RJ, Splinter E, Grosveld F, de Laat W (2002) Looping and interaction between hypersensitive sites in the active beta-globin locus. *Mol Cell* **10**: 1453–1465.

Verschure PJ, van Der Kraan I, Manders EM, van Driel R (1999) Spatial relationship between transcription sites and chromosome territories. *J Cell Biol* **147**: 13–24.

Volpi EV, Chevret E, Jones T *et al.* (2000) Large-scale chromatin organization of the major histocompatibility complex and other regions of human chromosome 6 and its response to interferon in interphase nuclei. *J Cell Sci* **113**: 1565–1576.

Walter J, Schermelleh L, Cremer M, Tashiro S, Cremer T (2003) Chromosome order in HeLa cells changes during mitosis and early G1, but is stably maintained during subsequent interphase stages. *J Cell Biol* **160**: 685–697.

Yokota H, van den Engh G, Hearst JE, Sachs RK, Trask BJ (1995) Evidence for the organization of chromatin in megabase pair-sized loops arranged along a random walk path in the human G0/G1 interphase nucleus. *J Cell Biol* **130**: 1239–1249.

Yokota H, Singer J, van den Engh GJ, Trask BJ (1997) Regional differences in the compaction of chromatin in human G0/G1 interphase nuclei. *Chromosome Res* **5**: 157–166.